DOI 10.1007/s11237-017-9488-8
Theoretical and Experimental Chemistry, Vol. 52, No. 6, January, 2017 (Russian Original Vol. 52, No. 6, November-December, 2016)

EFFECT OF PHASE COMPOSITION OF SUPERCONDUCTOR $Y_3Ba_5Cu_8O_{18+\delta}$ ON ITS CONDUCTING CHARACTERISTICS

A. O. Pilipenko, S. A. Nedilko, A. G. Dziazko, and I. V. Fesich

UDC 546.43'56'64+538.945

*The effect of the method of synthesis on the crystallographic parameters, electrical properties, and oxygen nonstoichiometry of superconducting cuprate with nominal composition $Y_3Ba_5Cu_8O_{18+\delta}$ was investigated. The samples were synthesized by a solid state reaction (sample **A**), by coprecipitation of the hydroxocarbonates (sample **B**), and by the sol–gel technique (sample **C**). According to data from X-ray diffraction (XRD) and the temperature dependence of the specific resistance a single-phase superconductor is formed in the sol–gel method and has the highest critical temperature for transition to the superconducting state (T_c = 95 K), whereas samples **A** and **B** contain impurity phases and have lower critical temperatures for transition (92 and 87 K, respectively).*

***Key words**: superconducting cuprates, solid state reaction synthesis method, coprecipitation method, sol–gel technique, X-ray diffraction, electrical characteristics, thermal analysis.*

High-temperature superconducting (HTSC) cuprates have been subjects of fundamental and applied investigations for more than 30 years. They have found widespread use in the creation of electric motors, high-power magnets, energy storage systems, and components of high-frequency and ultrasensitive electronic devices [1].

It should be noted that four superconducting compounds in the Y–Ba–Cu–O system are known, namely: $YBa_2Cu_3O_{7-\delta}$ (Y-123), $YBa_2Cu_4O_{8-\delta}$ (Y-124), $Y_2Ba_4Cu_7O_{14+\delta}$ (Y-247), and $Y_3Ba_5Cu_8O_{18+\delta}$ (Y-358). There are a large number of intermediate non-superconducting cuprates, of which the most thermodynamically stable are $BaCuO_2$ and Y_2BaCuO_5 (the so-called "green phase" or Y-211). The crystal chemical structure of the superconductors of the above-mentioned system is characterized by the presence of a layered perovskite-like structure with different numbers of crystallographic planes (subsequently referred to as planes in the text), denoted as CuO_2, and CuO chains, and different mutual dispositions (δ is the oxygen nonstoichiometry index; the conventional notation of the HTSC cuprates is given in parentheses) [2, 3].

The structure of the unit cell of Y-123 can be represented as a block that contains parallel crystallographic planes: CuO, BaO, and CuO_2 (straight fragment, subsequently referred to in the text as fragment) and a mirror-inverted fragment in reverse order: CuO_2, BaO, and CuO (inverted fragment). The two fragments are separated by an yttrium atom [4]. The structure of Y-124 consists of two identical blocks with alternate straight and inverted fragments. These blocks are separated by two yttrium atoms located on opposite faces of the unit cell. Compound Y-247 contains in its structure a Y-123 block with a straight fragment, a Y-124 block, and a Y-123 block. In other words, alternate straight and inverted fragments are observed. Here all the CuO_2 planes are separated from each other by yttrium atoms, which is typical of all the superconducting phases described above. The cuprate Y-358 has a more complex structure and represents inverted and straight fragments separated by a BaO

Taras Shevchenko National University of Kyiv, Vul. L'va Tolstoho, 12, Kyiv 01033, Ukraine. E-mail: pilipenko.anastasiya@yandex.ua. Translated from Teoreticheskaya i Éksperimental'naya Khimiya, Vol. 52, No. 6, pp. 342-347, November-December, 2016. Original article submitted November 29, 2016; revision submitted December 5, 2016.

plane, beneath which lies a CuO_2 plane separated from the previous inverted and the next straight fragments by yttrium atoms, below which there are additional BaO and CuO_2 planes [5]. It was confirmed experimentally that the temperature of the transition to the superconducting state increases with increase in the number of crystallographic CuO_2 planes per unit cell in the Y-containing copper HTSCs [6].

To date intensive investigations have been carried out on the HTSC compounds R-247, where R = Y (T_c = 92 K), Pr (10-16 K), Er (89 K), Dy (60 K) [7-9], and R-358, where R = Y ($T_c \approx$ 100 K) [10, 11], Sm (92.5 K), Nd (91.1 K) [12], and Gd (100 K) [13].

The scientific interest in the cuprates R-358 arises from the relative simplicity of their synthesis and the high critical temperature of the transition to the superconducting state ($T_c \approx$ 100 K), which is higher for example than for the Y-123 ($T_c \approx$ 93 K) widely used in industry [11].

According to the literature the Y-358 superconductors are produced mainly by the ceramic method from a mixture of metal oxides [11, 14-19] and by the sol–gel technique [20-22]. There are no data in the literature on the possibility of producing Y-358 by other methods.

In this connection it seemed timely to establish a relationship between the method of synthesis, the chemical composition, and the properties for the case of the production of the superconductor Y-358 by coprecipitation of hydroxocarbonates (HOC) and hydroxooxalates (HOO) and also by the solid state reaction (SSR) and sol–gel (SG) methods, to determine the optimum conditions for the creation of superconducting ceramics, and to discover the processes that occur during the synthesis of the HTSC phase.

The aim of the work was to establish the effect of the methods of synthesis on the crystallographic parameters, electrical characteristics, and acid nonstoichiometry of the cuprate Y-358.

EXPERIMENTAL

The superconducting ceramic was synthesized by the HOC method and also by the SSR and SG methods.

SSR Method (Sample A). The starting compounds were yttrium oxide Y_2O_3 (“special purity 9-2”), copper oxide CuO (“chemical purity”), and barium carbonate $BaCO_3$ (“chemical purity”).

Yttrium and copper oxides and barium carbonate in stoichiometric proportions were rubbed to a uniform mass in an agate mortar.

HOC Method (Sample B). The charge for the synthesis of Y-358 was obtained by coprecipitation from aqueous solutions of yttrium (“chemical purity”), copper (“chemical purity”), and barium (“chemical purity”) nitrates mixed in stoichiometric proportions with a unimolar solution of Na_2CO_3 (“chemical purity”) in a molar ratio of 1 : 1.75. The precipitation was performed with intense agitation on a magnetic stirrer. After standing and aging for three days the mother solution was tested for the absence of yttrium, barium, and copper ions by qualitative analysis. The precipitate was then filtered off and washed with distilled water to a negative reaction for sodium cations (reaction with zinc-uranyl acetate). The color of the obtained yttrium, barium, and copper HOC was light-blue. The precipitation products were dried in air and rubbed in an agate mortar.

SG Method (Sample C). Stoichiometric amounts of titrated solutions of yttrium (“chemical purity”), barium (“chemical purity”), and copper (“chemical purity”) nitrates were mixed in a glassy graphite cup. Citric acid monohydrate (“chemical purity”) was used as gelling agent. Ammonia solution (“chemical purity”) with a concentration of 1.5 M was added to the reaction mixture to maintain a pH value of 6. The solution was slowly evaporated on a water bath until a uniform gelatinous mass was formed, and this was then dehydrated and calcined with gradual heating to 400 °C.

Thermal investigations were undertaken in order to determine the optimum temperatures for heat treatment of the charge material obtained by the methods outlined above. Thermal analysis was carried out on a synchronous STA 449 F1 Jupiter analyzer produced by the German firm Netzsch. The experiment was carried out in air with a constant heating rate of 10 °C/min, and the sample weight was 10 mg.

To produce the ceramic the polycrystalline powder after heat treatment was compressed into tablets 15 mm in diameter and 1-2 mm thick under a pressure of 100 MPa. The obtained tablets were held in air for 10 h at 900 °C (samples **A** and **C**) and at 800 °C (sample **B**) with intermediate grinding and compression after heating for 5 h.

The phase composition and the crystal lattice parameters of the obtained compounds were determined by X-ray powder diffraction on a Shimadzu LabX XRD-6000 diffractometer (CuK_α radiation, $\lambda = 0.15406$ nm, angle range $5° \le 2\theta \le 90°$). The recording rate was 2°/min. The phases were identified against the data base of the International Joint Committee of Powder Diffraction Standards (JCPDS PDF-2). The X-ray patterns were indexed, the space groups were determined, and the crystallographic parameters were calculated by means of the INDEX and X-Ray software.

The specific electric resistance of the samples was measured by a four-contact method on a Pillar-1UM instrument in the temperature range of 300-77 K.

The active oxygen content was determined in two stages using the iodometric titration method described in [23].

RESULTS AND DISCUSSION

The data from thermal analysis of the charge mixtures for samples **A**, **B**, and **C** were analyzed in order to establish the decomposition characteristics of the charge and to determine the temperature ranges for the synthesis of the Y-358 cuprate. The thermograms of the samples are presented in Fig. 1.

In the case of the SSR method it is possible to detect three weight loss sections on the TG curve in the region of 25-900 °C (see Fig. 1a). Water residues are removed and traces of yttrium hydroxocarbonate are decomposed in the regions of 80-100 and ~325 °C, respectively. Decomposition of the barium carbonate begins at 810 °C, as shown by the observed strong endo effect ($\Delta H = -23.4$ J/g) on the DSC curve and a marked change of weight on the TG curve.

Sample **B** loses the extraspherical water in the temperature range of 25-220 °C (Fig. 1b). The weight loss of the sample here amounts to 5%. The presence of exo effects in the region of 400-700 °C is due to the formation of yttrium dioxomonocarbonate and monooxodicarbonate and also copper monooxocarbonate. These intermediate compounds are thermally unstable and decompose with further increase of temperature. This is indicated by a broad endo effect in the region of 400-650 °C, which corresponds to the removal of CO_2. The total weight loss of the sample (Δm) amounts to 22.3%.

In order to remove the products from partial decomposition of the organic component the charge for the production of sample **C** was first calcined at 400 °C, after which a DSC/TG analysis was undertaken. On the TG curve (Fig. 1c) it is possible to see three sections in the temperature range of 25-960 °C on which there are endo effects accompanied by weight loss.

The region of weight loss in the range of 50-250 °C is probably due to removal of adsorbed water of crystallization ($\Delta m \approx 0.6\%$) that appeared after the charge was kept in air for three days. The second observed region of weight loss is in the range of ~600-870 °C ($\Delta m \approx 11\%$), which evidently corresponds to decomposition of the barium carbonate as a result of chemical interaction of the components of the charge. The last region of weight loss recorded at ~950-960 °C, probably, corresponds to partial removal of oxygen from Y-358.

Apart from the endo effects accompanied by weight losses, there is an exo effect on the DSC curve that can be attributed to crystallization of the superconducting phase. Thus, it can be concluded from the experimental data that the superconducting cuprate Y-358 is formed in the range of 870-890 °C.

On the basis of the data from the thermal investigations the obtained charge was placed in porcelain crucibles. Sample **A** was calcined at 900 °C for 24 h, sample **B** was subjected to stepwise heat treatment at 800 °C for 36 h and intermediately ground in an agate mortar after 12 and 24 h heat treatment, respectively, and sample **C** was heated from 400 to 800 °C with oven heating rate of 100 °C/h in order to prevent ignition and ejection of the charge containing a significant amount of organic mass from the crucible. It was then held at 800 °C for 24 h.

It should be noted that an attempt was made to synthesize the cuprate Y-358 by coprecipitation of the hydroxooxalates of the respective metals. However, it was not possible to obtain the compound; only reflections corresponding to the Y-211 and CuO phases were recorded on the X-ray pattern.

From the results of XRD it was established that only sample **C**, for which diffraction reflections of impurity phases were not detected on the diffractogram, is single-phased (Fig. 2a). Here, peaks belonging to Y-211 (JCPDS-PDF-2 card No. 80-0770) and CuO (JCPDS-PDF-2 card No. 65-2309) were recorded for samples **A** and **B**. The formation of the Y-211 phase on the surface of the tableted samples and also on the walls of the crucible in which the synthesis was conducted indicates a diffusion mechanism for decomposition of the charge. From the powder X-ray diffraction data it was established that the main

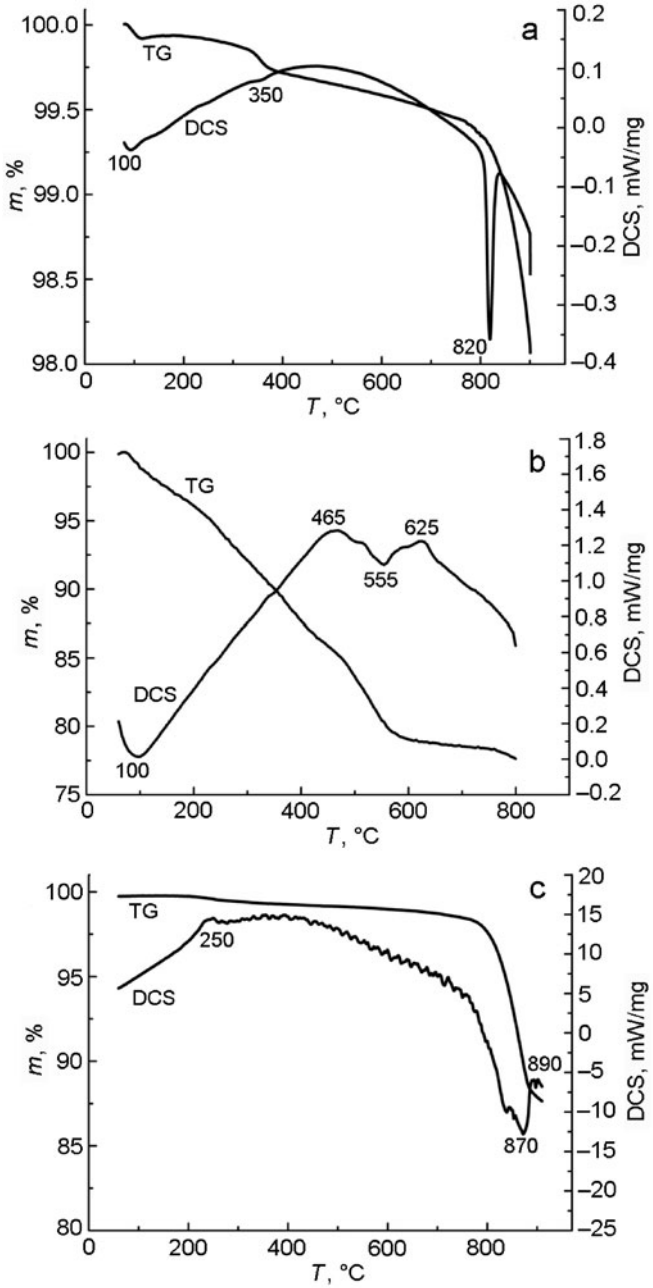

Fig. 1. Thermograms of the charge for synthesis of the compound $Y_3Ba_5Cu_8O_{18+\delta}$ by the SSR method (a), the HOC method (b), and the SG method (c).

Y-358 phase crystallizes in the orthorhombic system (space group *Pmm*2) in all the samples. Indexing of the reflections and calculation of the crystallographic parameters (Table 1) showed that the values of *a* and *b* for the three samples are close to the periods of the crystal lattice of the supercoducting Y-123 phase while the parameter *c* is approximately three times greater than *a* and *b*, which agrees well with published data [5].

From the investigations of the chemical composition–structure–property relationship for the copper-containing HTSC cuprates it was established that the optimum concentration of charge carriers in the CuO_2 layers of the superconductors with *p* conductivity lies in the range of formal degrees of oxidation of copper between +2.05 and +2.25 [24]. The results that we

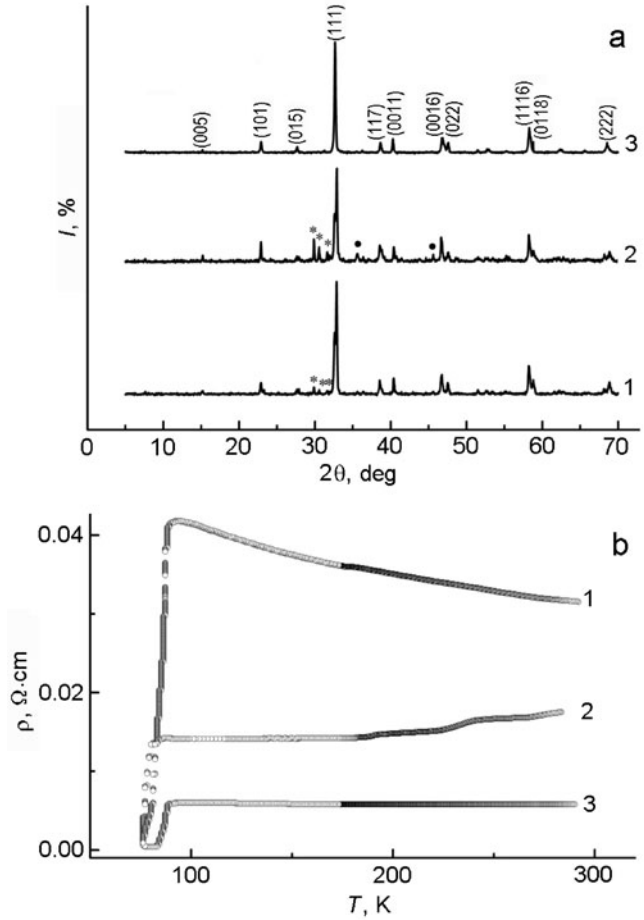

Fig. 2. Diffractograms (a) and temperature dependences of the specific electric resistance (b) of the compound $Y_3Ba_5Cu_8O_{18+\delta}$ produced by the SSR method (1), by the HOC method (2), and by SG method (3): * Y-211, • CuO.

obtained do not contradict the hypothesis presented above: for samples **A** and **C** the average degree of oxidation of copper is $n = 2.20$ whereas for sample **B** $n = 2.18$.

As follows from the electroneutrality principle, the equation for calculating the total oxygen content ($y \equiv 18 + \delta$) for the cuprate has the following form:

$$3\cdot(+3) + 5\cdot(+2) + 8(+n) + y\cdot(-2) = 0 \Rightarrow y = 1/2[8n + 19],$$

i.e., $y = 18.30$ for samples **A** and **C**, and $y = 18.22$ for **B**.

The decrease of the total oxygen index y and the average degree of oxidation of copper Cu^{n+}, observed for sample **B**, may be due to charge disordering in the cationic and oxygen sublattices of structure Y-358.

Figure 2b shows the graph for the temperature dependence of the specific resistance of the samples obtained by the three different methods. In the normal state the specific resistance ρ of sample **A** hardly changes at all with temperature, but there is a weak semiconductor dependence ($d\rho/dT < 0$) with $\rho_{298} = 3.15\cdot10^{-2}$ Ω·cm. In turn, for the superconducting cuprates obtained by the chemical homogenization methods (HOC and SG) ρ_{298} is smaller and amounts to $1.75\cdot10^{-2}$ Ω·cm (sample **B**) and $5\cdot10^{-3}$ Ω·cm (sample **C**). In addition, samples **B** and **C** exhibit metallic type of conductivity at $T < T_c$ ($d\rho/dT \geq 0$). The high

TABLE 1. Phase Composition and Unit Cell Parameters of the Superconducting Cuprate Y-358

Sample	Presence of impurity phases, %	Unit cell parameters			
		a, Å	*b*, Å	*c*, Å	*V*, Å^3
A	6% Y-211	3.849(2)	3.923(2)	31.055(9)	468.9(8)
B	17% Y-211, 8% CuO	3.817(6)	3.905(6)	31.123(4)	464.0(2)
C	–	3.850(1)	3.921(1)	31.033(6)	468.5(0)

TABLE 2. Critical Temperatures for Transition to the Superconducting State for the Sample $Y_3Ba_5Cu_8O_{18+\delta}$

Sample	T_c^{on}, K	T_c^{off}, K	ΔT_c, K
A	92	77	15
B	87	77	10
C	95	84	11

electric conductivity of samples **B** and **C** may be due to a contribution from conductivity at the intercrystallite grains on account of their high dispersivity. The data from low-temperature measurement of the specific electric resistance indicate that the temperature at the beginning of the transition to the superconductive state T_c^{on} = 87 K for sample **B** is significantly lower (Table 2) than for samples **A** and **C**, for which T_c^{on} = 92 and 95 K, respectively. The high temperature for the beginning of the transition to the superconducting state in the sample produced by the SG technique may be due to the single-phase nature of the sample (on account of chemical homogenization at the molecular level at the production stage). During analysis of the graphical relationships for specific resistance it was found that the width of the supercoducting transition $\Delta T_c = T_c^{on} - T_c^{off}$ for the compound $Y_3Ba_5Cu_8O_{18+\delta}$ amounts to 10, 15, and 11 K for samples **A**, **B**, and **C**, respectively.

The thermal transformations for the compound $Y_3Ba_5Cu_8O_{18+\delta}$ synthesized by three different methods have been investigated by thermogravimetric analysis. The results have shown that the unit cell parameters of the samples synthesized by the SSR and SG methods are similar, while their slight differences are explained by the presence of defects in the solid-phase sample. The single-phase nature of **C** in contrast to the other two samples was confirmed by X-ray diffraction. From the data of the resistance measurements it was established that all the samples are superconductors, but it must be pointed out that sample **A** has a semiconductor relationship in the specific resistance up to the temperature of the transition to the superconducting state, while the other two samples have a metallic relationship. Sample **C** has the highest temperature of transition to the superconducting state (about 95 K) and the chemical composition $Y_3Ba_5Cu_8O_{18.3}$ with unit cell parameters a = 3.850(1) Å, b = 3.921(1) Å, c = 31.033(6) Å in the orthorhombic system (space group *Pmm*2). The optimum conditions for the production of Y-358 are obtained with calcination of the charge produced by the SG method and held at 800 °C for 24 h and at 900 °C for 10 h in air. In spite of the fact that the oxygen indices for samples **A** and **C** are practically identical, the largest decrease in specific resistance is observed for sample **A** against sample **C**, which has the smallest decrease of specific resistance of the three investigated samples. In addition, it should be noted that significantly less time was spent on the synthesis of the sample

produced by the SG method than on the production of the other two samples. In view of the results that we have obtained it seems clear that the SG method is the best method for the synthesis of the superconducting cuprate with nominal composition $Y_3Ba_5Cu_8O_{18+\delta}$.

REFERENCES

1. S. A. Nedyl'ko, O. G. Dzyaz'ko, and M. A. Zelen'ko, *High-Temperature Superconductivity* [in Ukrainian], VPTs Kyiv University, Kyiv (2010).
2. U. Topal and M. Akdogan, *J. Supercond. Nov. Magn.*, **24**, No. 5, 1815-1820 (2011).
3. G. F. Voronin and S. A. Degterov, *Physica C*, **176**, Nos. 4-6, 387-408 (1991).
4. C. Park and R. L. Snyder, *J. Am. Ceram. Soc.*, **78**, No. 12, 3171-3194 (1995).
5. S. Gholipour, V. Daadmehr, A. T. Rezakhani, et al., *J. Supercond. Nov. Magn.*, **25**, No. 7, 2253-2258 (2012).
6. S. Nakajima, M. Kikuchi, Y. Syono, et al., *Physica C*, **158**, No. 3, 471 (1989).
7. J. L. Tallon, D. M. Pooke, R. G. Buckley, et al., *Phys. Rev. B*, **41**, No. 10, 7220-7723 (1990).
8. T. Fukushima, S. Horii, H. Ogino, et al., *Appl. Phys. Express*, **1**, No. 11, 111701-111702 (2008).
9. A. Matsushita, K. Fukuda, Y. Yamada, et al., *Sci. Technol. Adv. Mater.*, **8**, No. 6, 477-483 (2007).
10. P. Udomsamuthirun, T. Kruaehong, T. Nilkamjon, et al., *J. Supercond. Nov. Magn.*, **23**, No. 7, 1377-1380 (2010).
11. A. Aliabadi, Y. A. Farshchi, and M. Akhavan, *Physica C*, **469**, No. 22, 2012-2014 (2009).
12. U. Topal, M. Akdogan, and H. Ozkan, *J. Supercond. Nov. Magn.*, **24**, No. 7, 2099-2102 (2011).
13. A. Aliabadi, Y. Akhavan-Farshchi, and M. Akhavan, *J. Supercond. Nov. Magn.*, **27**, No. 3, 741-748 (2014).
14. T. Kruaehong, *Int. J. Phys. Sci.*, **9**, No. 16, 360-367 (2014).
15. S. Sujinnapram, P. Udomsamuthirun, T. Kruaehong, et al., *Bull. Mater. Sci.*, **34**, No. 5, 1053-1057 (2011).
16. A. Heidari, S. Vedad, N. Heidari, et al., *Materials*, **5**, No. 5, 882-888 (2012).
17. A. Esmaeili, H. Sedghi, M. Amniat-Talab, et al., *Eur. Phys. J. B*, **79**, No. 4, 443-447 (2011).
18. N. Akduran, *J. Low Temp. Phys.*, **168**, Nos. 5/6, 323-333 (2012).
19. S. Kutuk, S. Bolat, C. Terzioglu, and S. Altintas, *J. Alloy Compd.*, **650**, No. 46, 159-164 (2015).
20. D. Wang, A. Sun, P. Shi, et al., *J. Supercond. Nov. Magn.*, **27**, No. 10, 2365-2369 (2014).
21. N. Zarabinia, V. Daadmehr, F. Shahbaz Tehran, et al., *Procedia Mater. Sci.*, **11**, 242-247 (2015).
22. M. Akyol, A. O. Ayaş, C. Akca, et al., *Bull. Mater. Sci.*, **38**, No. 5, 1231-1237 (2015).
23. I. V. Fesych, S. A. Nedil'ko, O. G. Dzyaz'ko, and V. V. Boklashchuk, *Fiz. Khim. Tverd. Tila*, **13**, No. 4, 977-982 (2012).
24. E. V. Antipov and A. M. Abakumov, *Usp. Fiz. Nauk*, **178**, No. 2, 190-202 (2008).